ARTICLE

Correlation between Surface Stress and Apparent Young's Modulus of Top-Down Silicon Nanowires

Giovanni Pennelli,* Massimo Totaro, and Andrea Nannini

Dipartimento di Ingegneria della Informazione, Università di Pisa, Via G. Caruso, I-56122 Pisa, Italy

ABSTRACT In this work, we report experimental evidence of surface stress effects on the mechanical properties of silicon nanostructures. As-fabricated, top-down silicon nanowires (SiNWs) are bent up without any applied force. This self-buckling is related to the surface relaxation that reaches an equilibrium with bulk deformation due to the material elasticity. We measure the SiNW self-deformation by atomic force microscopy (AFM), and we apply a simple physical model in order to give an estimation of the surface stress. If the equilibrium is altered by a nanoforce, applied by an AFM tip, nanowires find a new equilibrium condition bending down (mechanical bistability). In this work, for the first time, we report a clear and quantitative relationship between the SiNWs' apparent Young's modulus, measured by force-deflection spectroscopy, and the estimated value of surface stress, obtained by self-buckling measurements taking into account the Young's modulus of bulk silicon. This is an experimental confirmation that the surface stress is fundamental in determining mechanical properties of SiNWs, and that the elastic behavior of nanostructures strongly depends on their surfaces.

Top–down Si Nanowire:
CLAMPED – BENDED

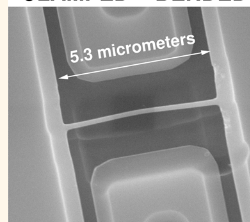

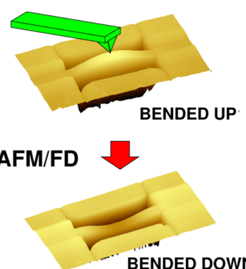

APPARENT Young's modulus: SURFACE EFFECTS

KEYWORDS: nanoelectromechanical system · nanoelasticity · nanobeam · surface stress · nanowire

Nanoelectromechanical systems are very important for their interesting applications in the field of advanced devices and sensing. To this end, in recent years, great efforts have been performed for the comprehension of the mechanical and elastic properties of materials at the nanometer scale. In particular, atomic force manipulation of nanowires,[1−3] pinned in a particular location, has been largely employed to measure the elastic (Young's) modulus Y of materials at reduced dimensionality. Several experimental works reported a strong variation of Y when the nanowire width is reduced. In fact, some of them reported a decrease of Y with the nanowire width decreasing,[1,2,4,5] while other works reported an increasing of Y.[3,6,7] As demonstrated by theoretical works on silicon and other materials,[8−10] material compliance should decrease at low nanometric scale. This means that the Young's modulus Y increases. However, the surface stress plays a prominent role: this is particularly true in nanowires due to the high surface-to-volume ratio.[10] The effect of surface stress on mechanical properties has been theoretically investigated for silicon[11] and metal[12] nanowires. Experimental works reported the effect of surface stress for silver[13,14] and lead nanowires.

In this work, we study mechanical deformations of high crystalline quality, top-down fabricated silicon nanowires released by means of BHF under-etching and doubly clamped in crystalline silicon. We ascribe these deformations that are in the elastic regime to surface relaxation. The surface reaches an equilibrium with the nanowire bulk; therefore, once fabricated, without any applied force, nanowires are buckled. If this equilibrium is perturbed, nanowires find a new equilibrium position bending in the opposite direction (mechanical bistability). In this work, for the first time, measurement of the SiNW self-buckling, performed by means of AFM imaging, has been used to give an estimation of the surface stress. Force-deflection spectroscopy is then performed in order to measure the SiNWs' apparent Young's modulus that was higher than the value for macroscopic silicon

* Address correspondence to g.pennelli@iet.unipi.it.

Received for review August 27, 2012 and accepted November 6, 2012.

Published online November 06, 2012
10.1021/nn304094b

© 2012 American Chemical Society

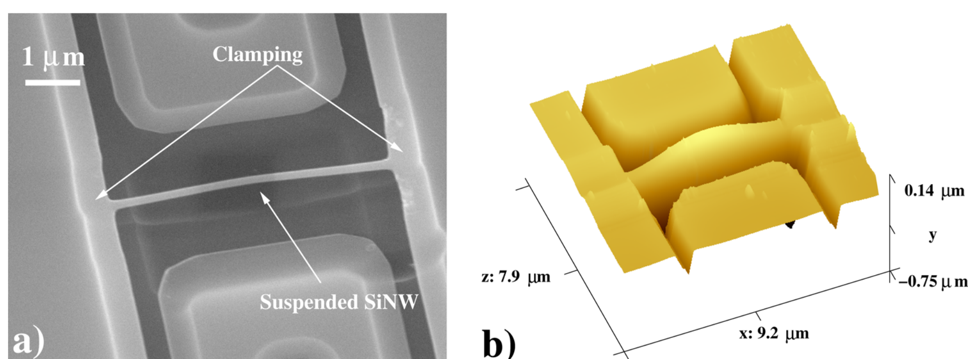

Figure 1. (a) SEM image of a typical SiNW after oxide under-etch, released from substrate and clamped at its extremities: the nanowire is bent up. (b) No-contact AFM image of a released SiNW.

structures. This higher experimental value is compatible with the surface stress that we estimated by measuring the SiNW self-buckling.

RESULTS AND DISCUSSION

Mechanical Self-Deformation of Silicon Nanowires. One of the most interesting techniques for nanomechanical characterization is the use of nanostressing applied by means of an atomic force microscope (AFM). Most of the works devoted to nanomechanical characterization show results obtained with bottom-up fabricated nanostructures, such as carbon nanotubes[15−17] or metal nanowires.[2] Several works are dedicated to bottom-up silicon nanowires, typically fabricated by vapor−liquid−solid (VLS) growth.[4,6] Once fabricated, a suitable mechanical clamping must be provided in order to immobilize these nanostructures and to allow nanomechanical stressing. In this work, we characterize top-down silicon nanowires fabricated by a process based on high-resolution electron beam lithography and stress-controlled oxidation reported in previous works.[18−20] Our top-down technique allows the simultaneous fabrication of nanowires and clamping regions. Therefore, at the end of the process, nanowires are already doubly clamped at their extremities. Furthermore, the clamping is of excellent quality because there is crystalline continuity between the clamping regions and the nanowire.

In the Methods section, we report a brief summary of the fabrication process. At the end of the process, the nanowires are suspended between the clamping regions. We used suitable oxidation times so that nanowires have a triangular (isosceles) cross section, delimited by two ⟨111⟩ surfaces on the sides and by a bottom ⟨100⟩ surface. Nanowires are exactly oriented in the ⟨110⟩ direction.

Figure 1a shows a SEM image of a typical suspended nanowire after the final reduction and BHF etch. In particular, a nanowire 5.3 μm long (distance between the clamping regions) and 150 nm wide (W = 150 nm) is shown. The image has been taken with a tilt of roughly 30° in order to better show the SiNW self-bending: the nanowire is deformed in a plane perpendicular to the wafer surface (vertically). We do not observe any deformation in the horizontal direction (parallel to the wafer surface). For an accurate measurement of the deformation, AFM images have been taken on several SiNWs both in contact and in no-contact mode; no significant differences have been detected between no-contact images and contact images taken with a low force (2 nN). Figure 1b shows a typical AFM image (no-contact mode) that highlights the SiNW deformation in a plane perpendicular to the wafer surface. Similar deformations have been observed in all of the fabricated samples, with nanowire widths W in the range of 120−160 nm. Although residual stress in SOI wafers can vary enormously, the top silicon layer should present mainly a tensile stress, as shown by several works.[21,22] Furthermore, as reported in ref 21, the residual tensile stress is relatively small in substrates with top layer thicknesses considered in our work. Phenomena that can induce a compressive stress must be considered in order to explain the bending of SiNWs. Theoretical works[10,11] have shown that the effect of the surface stress is to elongate unconstrained SiNWs. The equilibrium length is reached when the energy released by the surface relaxation is equivalent to the mechanical energy stored in the elongated nanowire bulk. This means that clamped nanowires undergo a compressive stress for the effect of surfaces. Bottom-up nanowires, considered by several works, are fabricated unconstrained and then clamped once their equilibrium length is reached. For this reason, without applied load, no self-deformations can be observed in bottom-up doubly clamped nanowires. Their surface strain can be detected only by measuring the effective Young's modulus that, for the surface effects, can be higher[13,14] with respect to macroscopic structures made of the same material. In the present work, the distance between clamping regions is fixed during all top-down fabrication steps; after releasing, the surface relaxes and tends to elongate the SiNW. This induces a compressive stress with a consequent bending of

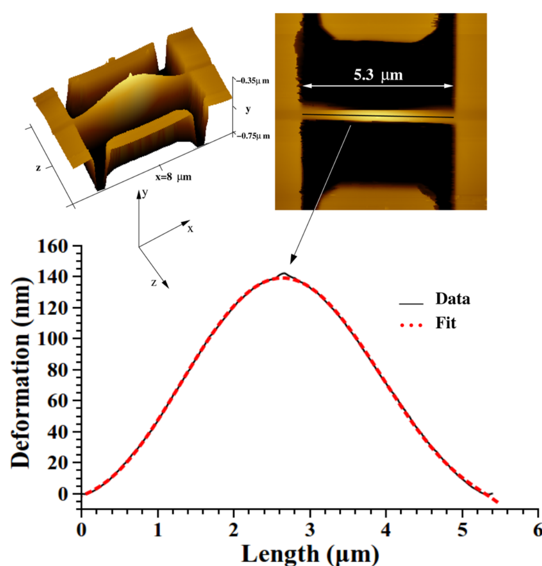

Figure 2. Main image: extracted SiNW profile (leveled) is shown, together with the sixth-order polynomial fit. Top left: AFM image of the released SiNW. Top right: pattern where the profile has been extracted is shown.

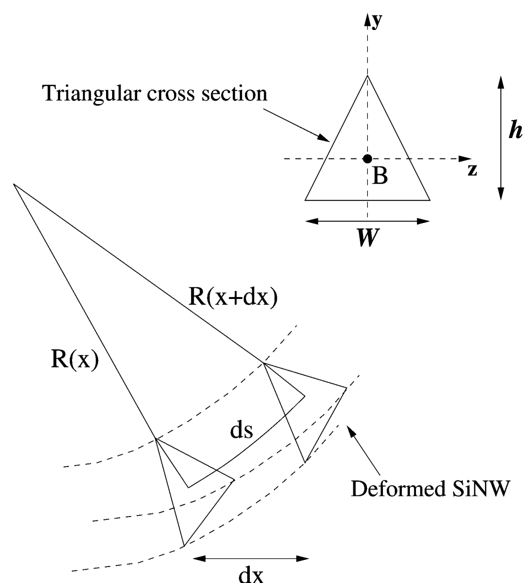

Figure 3. Sketch of a deformed nanowire with triangular cross section (top right). The deformation radius $R(x)$ and its reciprocal $\chi(x)$ can be determined by the polynomial fit.

the SiNW. Our SiNWs are bent in the vertical direction (perpendicular to the surface) because the momentum of inertia of a triangular isosceles cross section is minimum with respect to the horizontal direction (base).

We measured the SiNW self-bending in order to give an estimation of the surface stress. To this end, a deformation profile of some typical SiNWs has been extracted from AFM contact (force of 2 nN) images. Figure 2 shows a typical longitudinal profile, extracted from the AFM image reported in the top right inset. The distance between the clamping regions, which is the original SiNW length, is L = 5.3 μm; the nanowire is 130 nm wide. The nanowire buckling δ in the middle resulted δ = 135 nm. The main graph shows the extracted deformation profile and a fit with a sixth-order polynomial, used as an analytical approximation of the nanowire deformation $v(x)$. This analytical approximation is used for the evaluation of the bulk elastic energy stored in the bent nanowire. This energy must be equal to the work done by the surface stress during the relaxation. The elastic regime is assumed in the data reduction (see the force-deflection measurements in the following section). For elastic deformations, the strain ε in the SiNW bulk can be expressed as a function of the curvature radius $R(x)$, $\chi(x) = 1/R(x)$, of the beam:[23]

$$\varepsilon(x, y) = \varepsilon_0 - \chi(x)y \tag{1}$$

where ε_0 is the axial deformation, which is the SiNW elongation, and y is referred to the triangular cross section center of mass B, as schematically shown in Figure 3. The reciprocal of the curvature radius $\chi(x) = 1/R(x)$ can be expressed as a function of the nanowire deformation $v(x)$:

$$\chi(x) = \frac{\frac{d^2v}{dx^2}}{\left(1 + \left(\frac{dv}{dx}\right)^2\right)^{3/2}} \tag{2}$$

The axial deformation ε_0 can be obtained calculating the elongated nanowire length L_1:

$$L_1 = \int_0^L \sqrt{1 + \left(\frac{dv}{dx}\right)^2}\, dx \tag{3}$$

$$\varepsilon_0 = \frac{L_1 - L}{L} \tag{4}$$

The values of $\chi(x)$, ε_0, and ε can be obtained by numerical derivatives of the measured profile. However, derivatives of experimental data are very unstable. For this reason, we estimated $\chi(x)$, ε_0, and ε by using analytical derivatives of the sixth-order polynomial fit of the experimental profile. The strain ε_0 is related to the bulk stress σ by the well-known relationship $\sigma = Y\varepsilon$. Following theoretical works,[11] confirmed by experimental measurements,[1,4] in the case of nanowires wider than 100 nm (our investigated range is W between 120 and 160 nm), the silicon bulk value can be assumed for Y, which for the $\langle 110 \rangle$ direction is Y = 169 GPa. The density of mechanical deformation energy is $\partial E_{bulk}/\partial V = 1/2\sigma\varepsilon = 1/2Y\varepsilon^2$. The total bulk elastic energy stored in the deformed nanowire can be obtained as

$$E_{bulk} = \int_V \frac{1}{2} Y \varepsilon(x, y)^2 dV \tag{5}$$

$$E_{bulk} = \int_L \int_A \frac{1}{2} Y \varepsilon(x, y)^2 dA dx \tag{6}$$

where V is the nanowire volume and A is the area of the nanowire triangular cross section ($dA = dydz$). In this way, the total bulk elastic energy stored in the nanowire can be determined as

$$E_{bulk} = \int_L \left(\int_{y,z} \frac{1}{2} Y(\varepsilon_0 - \chi(x)y)^2 dydz \right) dx \qquad (7)$$

Making some simple calculations, it is easy to demonstrate that this integral can be written as

$$E_{bulk} = \frac{1}{2} Y \varepsilon_0^2 + \frac{1}{2} YJ \int_x \chi^2(x) dx \qquad (8)$$

where J is the moment of inertia of the triangular section $J = Wh^3/36$. At this point, the mechanical energy stored in the bulk of the deformed nanowire can be estimated on the basis of experimental data: $\chi(x)$ is easily calculated using eq 2 by using for $v(x)$ the sixth-order polinomial fit; then, $\chi(x)$ is used for a numerical evaluation of the integral in expression 8). This evaluated energy must be equal to the work done by the surface during its relaxation. For small deformations, the relationship between surface stress τ and surface strain can be approximated by a linear law:[14,24−26]

$$\tau = \tau_0 + Y_S \varepsilon \qquad (9)$$

The energy associated with the work done by the surface stress can be expressed as

$$E_S = \int_S \left(\tau_0 \varepsilon + \frac{1}{2} Y_S \varepsilon^2 \right) dS \qquad (10)$$

where S is the lateral surface of the silicon nanowire. In order to perform this calculation, some approximations must be done. At first, let us assume that the second term, containing $\varepsilon^2 \ll \varepsilon$ ($\varepsilon \ll 1$), can be neglected; this should be acceptable for a rough estimation. Furthermore, surface stress is anisotropic and depends on the surface orientation. In the present case, the triangular nanowire is delimited by a $\langle 100 \rangle$ surface on the bottom and two $\langle 111 \rangle$ surfaces on the two sides; our procedure does not allow to distinguish between the three surfaces; therefore, only an estimation of the average value of τ_0 on all lateral surfaces can be given. The integral in 10 can be rewritten as

$$E_S = \int_S \tau_0 \varepsilon dS$$

$$E_S = \int_0^L \left(\int_P \tau_0 \varepsilon dP \right) dx$$

where P is the perimeter of the nanowire cross section with area A. The surface stress ε can be calculated by means of the expression 1, where this time y must be taken on the border (perimeter) of the triangular cross section. Our cross section is defined by the KOH anisotropic etching, with base W and $h = W/2\sqrt{2}$ fixed by the etching properties. Some simple mathematical steps allow expression of the above integral as

$$E_S = \tau_0 \left(\varepsilon_0 PL - w^2 \sqrt{2} \frac{\sqrt{3} - 2}{12} \int_0^L \chi(x) dx \right) \qquad (11)$$

where again ε_0 and $\int_0^L \chi(x)dx$ can be evaluated by the polynomial sixth-order approximation of the experimental nanowire profile. By imposing

$$E_{bulk} = E_S \qquad (12)$$

and using eqs 11 and 8, we obtain τ_0

$$\tau_0 = Y \frac{\frac{1}{2} \varepsilon_0^2 + \frac{1}{2} J \int_x \chi^2(x) dx}{\varepsilon_0 PL - W^2 \sqrt{2} \frac{\sqrt{3} - 2}{12} \int_0^L \chi(x) dx} \qquad (13)$$

In the case of the nanowire shown in Figure 2, the procedure (profile extraction from AFM image, fitting with a sixth-order polynomial, numerical integration of integrals in eq 13) has been repeated starting from four different images of the same nanowire. The estimated τ_0 value is $\tau_0 = 3.67 \pm 0.02$ J/m^2, with W = 130 nm measured by SEM inspection.

Although this value is a first-order approximation, averaged on nanowires' sides (different crystalline planes), it gives a good agreement with other mechanical characteristics of SiNWs, as shown in the following subsection. The estimated τ_0 value is strongly dependent on the nanowire width because W appears both in the expression of inertia momentum J and, explicitly, in eq 13. Therefore, τ_0 is quite affected by errors in the measurement of W. If, for example, an error of ± 5 nm is considered on the measurement of W = 130 nm, τ_0 assumes the values of 3.46 J/m^2 for W = 125 nm and 3.93 J/m^2 for W = 135 nm. The whole procedure has been repeated for several AFM images taken on five different nanowires, with W in the range of 120−160 nm measured by SEM inspection. All values were in good agreement, in the range of 3.5−4.2 J/m^2. This is a strong indication that the main cause of silicon nanowire deformation is the surface stress that scales as the cross section perimeter, and that eventual residual volume stress, scaling as the cross section area, gives only a small contribution. The surface stress values that we found are comparable but slightly higher than the ones numerically evaluated by theoretical works,[10,11] which are between 0.5 and 2 J/m^2 depending on surface conditions. In preliminary experiments, we found that the surface stress value depends on the treatments performed on the SiNW and, in particular, on the oxidation times and temperatures for which the state of the surface can be very different with respect to the one analyzed in theoretical works.

Force/Deflection and Apparent Young's Modulus of Silicon Nanowires. We applied a force of few tens of nanonewtons on the SiNWs by means of the AFM tip, in order to

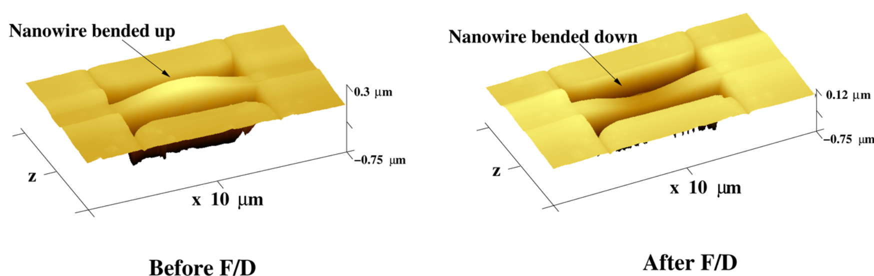

Figure 4. AFM images before and after F/D measurement. The change on the nanowire bending is evident. Both images have been taken in contact mode with a force of 2 nN that gives a negligible nanowire deformation.

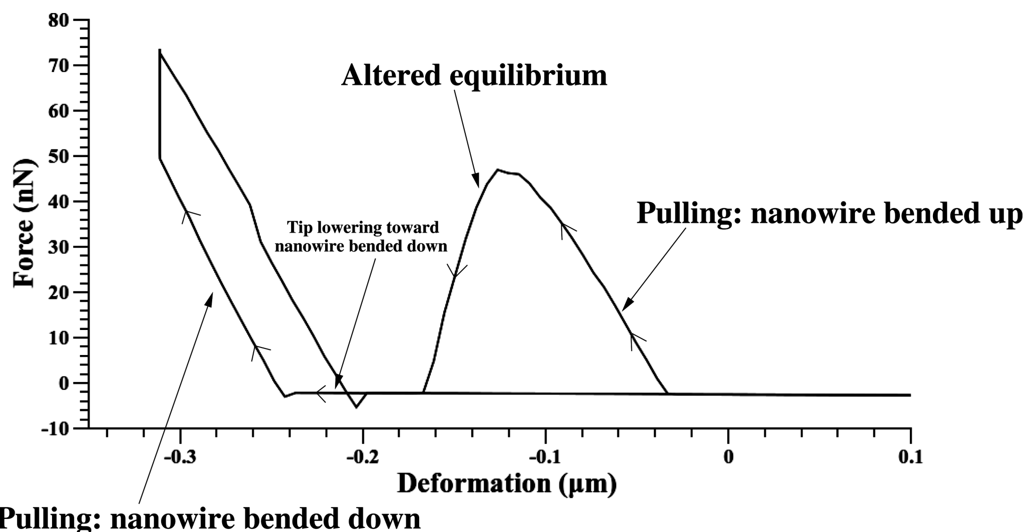

Figure 5. Typical F/D curve of a nanowire, originally deformed with a negative concavity ("bended up").

perform force-deflection measurements (F/D spectroscopy) and to measure the apparent Young's modulus of SiNWs. We observed that the applied force can modify the mechanical equilibrium of the bent up SiNW. If the deviation from equilibrium is sufficiently high, after an unstable phase, the nanowire reaches a new equilibrium condition with a different deformation. Figure 4 shows AFM images of a typical nanowire, taken immediately before and immediately after the application of a force in the middle. F/D measurements, recorded during the application of the force, are shown in Figure 5. From Figure 4, we can see that the nanowire changed its deformation state during the F/D measurement, from "bent up" (negative concavity) before the F/D characterization to "bent down" (positive concavity) after the F/D. To our knowledge, this behavior has never been observed before. As described in the previous section (see also Figure 4 "Before F/D"), once fabricated and suspended, the silicon nanowire bulk is in mechanical equilibrium with its surface and the nanowire is bent up. The first part of the F/D curve (see Figure 5 right part) shows that, for low applied force, the nanowire deformation is proportional to the force; that is, the deformation is linear, and the nanowire is in the elastic regime. When the force is sufficiently high (around 40 nN in the case of Figure 5), the mechanical equilibrium is altered: the nanowire becomes unstable and reaches a new equilibrium position bending down. At this point, the AFM tip is not more in contact with the nanowire, and it must go down to be applied again: see the flat curve between the right part and the left part in Figure 5. Once the bent down nanowire is reached, the tip again applies its force and the nanowire deformation increases: see the left part (linear) of Figure 5. Note that once the nanowire has found a new equilibrium condition "bent down", the relationship between force and deformation is still linear: this demonstrates that the nanowire mechanical behavior is always in the elastic regime.

Once the nanowire has reached its new equilibrium position, bent down, we positioned again the tip in the middle and repeated the F/D measurement in order to determine the apparent Young's modulus. To do that, we followed the procedure reported in ref 2. The deformation $\delta = v(L/2)$ with a force applied in $L/2$ is evaluated by using a comparison F/D curve taken on the bulk material. Figure 6 shows a sketch of the measurement procedure. Two F/D curves are recorded, one with the tip positioned on the bulk material and the other with the tip positioned in the middle ($L/2$) of the nanowire. The ratio between deformation and

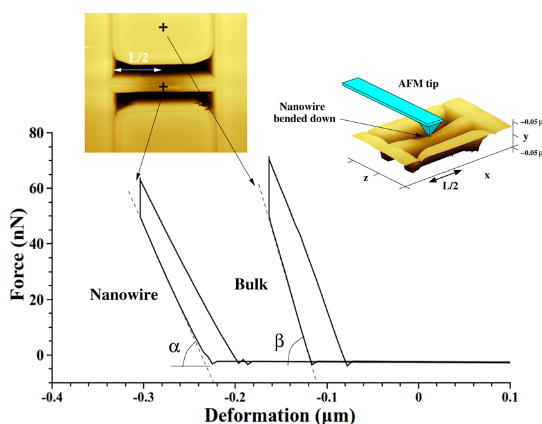

Figure 6. F/D curves, measured positioning the AFM tip as shown in the inset. The two values, tan α and tan β, are measured by means of a linear fit in the region of interest, as shown by the dashed lines. The F/D curves have been measured once the nanowire is bent down.

applied force δ/f can be determined as

$$\frac{\delta}{f} = \frac{\tan\beta - \tan\alpha}{\tan\beta\tan\alpha} \qquad (14)$$

In the present case, the nanowire is in equilibrium, already deformed before the application of the force. The δ, evaluated by F/D, is the increase of the deformation with respect to the equilibrium condition, due to the applied force. For the case of the data presented in Figure 6 ($W = 130$ nm, $L = 5.3$ μm), we found $\delta/f = 0.542$ m/N. The deformation/force ratio of a beam in the elastic regime, with a load positioned at $L/2$, is well-known,[23] and it is

$$\frac{\delta}{f} = \frac{1}{192}\frac{L^3}{JY} \qquad (15)$$

This formula, together with the experimental measurement of δ/f, allows determination of the apparent Young's modulus Y ($Y_{apparent}$) of our nanowire. Specifically, for the data shown in Figure 6, it gives $Y_{apparent} =$ 510 GPa, which is higher than the bulk Young's modulus for silicon in the ⟨110⟩ direction (that is, 169 GPa). This high value of the apparent Young's modulus can be explained by considering the surface effects because the applied force modifies both the bulk and the surface of the SiNW. With respect to the equilibrium, the applied force changes the total mechanical energy stored in the nanowire of an amount ΔE_{stored} that is given both by the contribution of bulk (ΔE_{bulk}) and by the contribution of surface (ΔE_S):

$$\Delta E_{stored} = \Delta E_{bulk} + \Delta E_S \qquad (16)$$

The variation of the internal stored energy must be equal to the elastic energy developed externally by the force. This external energy is a half of the total work done by the force itself:

$$E_{force} = \frac{1}{2} f\delta = \Delta E_{stored} \qquad (17)$$

For example, in the case of the F/D shown in Figure 6 ($\delta/f = 0.542$ m/N), if a force of 40 nN is used for the calculation, we have $\delta = 22$ nm. The energy developed by the force is $E_{force} = 1/2f\delta = 4.34 \times 10^{-16}$ J.

The nanowire is in the elastic (linear) regime; therefore, the superposition principle can be used in order to make an easier evaluation. Following this principle, the deformation due to the applied force can be treated separately from the self-deformation. When we consider only the deformation due to the applied force, $\Delta E_{stored} = 0$ for force = 0. In this way, the variation of the elastic energy ΔE_{stored} can be simply written as

$$\Delta E_{stored} = E_{stored} = E_{bulk} + E_S \qquad (18)$$

This stored energy should be equal to $E_{force} = 1/2f\delta$. The energies stored as elastic deformation of the bulk E_{bulk} and of the surface E_S can be evaluated by considering the well-known expression of the factor $\chi(x)$ for a doubly clamped beam with a force applied at $L/2$:

$$\chi(x) = \frac{24\delta(L - |L/2 - x|)}{L^3} \qquad (19)$$

In this expression, δ is the deformation for $x = L/2$, which is the quantity obtained by the F/D measurement. This expression can be used for a numerical evaluation of the integrals for the bulk energy and for the surface energy reported in the previous section:

$$E_{bulk} = \frac{1}{2} Y(\varepsilon_0^2 + J\int_x \chi^2(x)\mathrm{d}x) \qquad (20)$$

$$E_S = \tau_0\left(\varepsilon_0 PL - W^2\sqrt{2}\frac{\sqrt{3}-2}{12}\int_0^L \chi(x)\mathrm{d}x\right) \qquad (21)$$

The standard bulk value of Y = 169 GPa (⟨110⟩ direction) is used for evaluating E_{bulk}. For the calculation of E_S, we used the value of τ_0 estimated from the self-deformation, as reported in the previous section. In the case of the F/D shown in Figure 6, by considering again a force of 40 nm, $\delta/f = 0.542$ m/N, $\tau_0 = 3.67$ J/m^2 (see previous section), we obtain the value E_{stored} = 4.32×10^{-16} J. This value is very close to the mechanical energy produced by the work of the force (see above): $E_{force} = 4.34 \times 10^{-16}$ J.

The whole procedure has been repeated for several nanowires. For each nanowire, the value of τ_0 has been evaluated by measuring its self-deformation. Then, a first F/D measurement has been used for bending down the nanowire. After that, we performed a second F/D measurement and evaluated δ/f. We always found a good agreement (within 10%) between variation of mechanical stored energy (bulk and surface) and work done by the applied force.

CONCLUSIONS

In conclusion, in this work, we demonstrate that the SiNW's apparent Young's modulus, determined by F/D

spectroscopy measurements, is consistent with the effects due both to the elastic deformation of the nanowire bulk and to the elastic strain of the surface. In particular, we measured the self-buckling of as-fabricated nanowires, by AFM imaging, and used these measurements to give an estimation of the surface stress τ_0. Then, we measured the apparent Young's modulus by F/D and found that it is higher than Y_{bulk}. Mechanical behavior of bulk silicon strongly depends on the crystallographic orientation. In our case, the process that we employed for the fabrication of nanowires is based on anisotropic etching, so that nanowires are oriented in the ⟨110⟩ direction: therefore, the value Y_{bulk} = 169 GPa has been considered. A simple model that takes into account both Y and surface stress τ_0 can be applied to the evaluation of the apparent Young's modulus of the nanowire. Following this model, we found that the measured higher value of Y is compatible with the bulk value Y_{bulk} and with the estimated value of surface stress.

We suggest that the value of the surface stress τ_0 is strongly dependent on the surface states and on the process steps used in the nanowire fabrication. In particular, τ_0 strongly depends on the oxidation conditions (temperature and time) that heavily affect the surface reconstruction. In future works, different process conditions and treatments will be investigated, and their eventual effects on surface stress will be studied.

METHODS

Top-Down Fabrication of Silicon Nanowires. The fabrication process is based on silicon-on-insulator (SOI) crystalline wafers with a ⟨100⟩-oriented, high crystalline quality (Czochralski), top silicon layer 260 nm thick. A 50 nm thick SiO_2 layer, to be used as a mask for the silicon etching, is grown by dry thermal oxidation and patterned by e-beam lithography, using a standard PMMA resist. After the SiO_2 etching and PMMA stripping, the top silicon layer is anisotropically etched using a KOH water solution (35% in weight) saturated with isopropyl alcohol (IPA) at 43 °C. The anisotropic etching stops on precise crystalline planes, defining a very regular trapezoidal cross section even on long wires. For effect of the etch, the SiNW is precisely oriented in the ⟨110⟩ direction. After the etch, we used a well-controlled oxidation process for reducing the SiNW width. In our previous works on SiNW fabrication,[19,20] we observed that the trapezoidal cross section becomes triangular after suitable oxidation times if the top width defined in the lithographic step is smaller than the thickness of the silicon top layer. Furthermore, as demonstrated by numerical simulations, the oxidation rate is reduced by the stress generated during the growth, resulting in a very good control of the final shape.

At this point, a buffered HF (BHF) etch (etch rate about 50 nm/min) is performed for more than 12 min. This etch time is sufficient to remove all of the grown SiO_2 and for under-etching the SiO_2 below the nanowire; at the end, the SiNW is suspended and clamped at its extremities. A last oxidation step is then performed for 10 min at 1150 °C for a further reduction of the nanowire; then, this last oxide layer is removed by BHF. At the end, the nanowire has a triangular cross section, delimited by a bottom ⟨100⟩ crystalline plane base, with a width W that depends on the width of the initial mask and on the oxidation reduction process. We used suitable oxidation times so that the final cross section is a isosceles triangle, delimited by two ⟨111⟩ planes on the sides that are parallel to the original planes defined by the anisotropic etching.

AFM and F/D Measurements. All of the AFM imaging and measurements have been performed by means of a PSIA XE-100 (Park Systems). No-contact images have been taken by a 135/30/4 μm cantilever (length/width/thickness), with a tip radius of about 10 nm and a resonant frequency of about 330 kHz. Contact images have been taken by a 130/35/1 μm cantilever (length/width/thickness), tip radius of about 10 nm, and force constant of 0.6 N/m.

The proprietary software XEP-PSIA has been used both for image acquisition (in tiff format) and for force/deflection measurements. F/D measurements have been acquired and saved in txt format and reduced by standard software for data analysis (Origin and/or QtiPlot). The profile extraction has been performed by means of Gwdyddion AFM image analysis software, saved in txt format and analyzed by Origin or QtiPlot, which have been used both for plotting and for performing the sixth-order polynomial fit.

Numerical integrations have been performed by suitable programs, developed for this work by implementing standard algorithms in C++ language.

Conflict of Interest: The authors declare no competing financial interest.

REFERENCES AND NOTES

1. Heidelberg, A.; Ngo, L. T.; Wu, B.; Phillips, M. A.; Sharma, S.; Kamins, T. I.; Sader, J. E.; Boland, J. J. A Generalized Description of the Elastic Properties of Nanowires. *Nano Lett.* **2006**, *6*, 1101–1106.
2. Xiong, Q.; Duarte, N.; Tadigadapa, S.; Eklund, P. C. Force-Deflection Spectroscopy: A New Method To Determine the Young's Modulus of Nanofilaments. *Nano Lett.* **2006**, *6*, 1904–1909.
3. Gordon, M. J.; Baron, T.; Dhalluin, F.; Gentile, P.; Ferret, P. Size Effects in Mechanical Deformation and Fracture of Cantilevered Silicon Nanowires. *Nano Lett.* **2009**, *9*, 525–529.
4. Zhu, Y.; Xu, F.; Qin, Q.; Fung, W. Y.; Lu, W. Mechanical Properties of Vapor−Liquid−Solid Synthesized Silicon Nanowires. *Nano Lett.* **2009**, *9*, 3934–3939.
5. Li, X.; Ono, T.; Wang, Y.; Esashi, M. Ultrathin Single-Crystalline-Silicon Cantilever Resonators: Fabrication Technology and Significant Speciment Size Effect of Young's Modulus. *Appl. Phys. Lett.* **2003**, *83*, 3081–3083.
6. Kizuka, T.; Takatani, Y.; Asaka, K.; Yoshizaki, R. Measurements of the Atomistic Mechanics of Single Crystalline Silicon Wires of Nanometer Width. *Phys. Rev. B* **2005**, *72*, 035333.
7. Tabib-Azar, M.; Nassirou, M.; Wang, R.; Sharma, S.; Kamins, T. I.; Islam, M. S.; Williams, R. S. Mechanical Properties of Self-Welder Silicon Nanobridges. *Appl. Phys. Lett.* **2005**, *87*, 113102.
8. Broughton, J. Q.; Meli, C. A.; Vashishta, P.; Kalia, R. K. Direct Atomistic Simulation of Quartz Crystal Oscillators: Bulk Properties and Nanoscale Devices. *Phys. Rev. B* **1997**, *56*, 611–618.
9. Lee, B.; Rudd, R. E. First-Principles Study of the Young's Modulus of Si 001 Nanowires. *Phys. Rev. B* **2007**, *75*, 041305.
10. Lee, B.; Rudd, R. E. First-Principles Calculation of Mechanical Properties of Si 001 Nanowires and Comparison to Nanomechanical Theory. *Phys. Rev. B* **2007**, *75*, 195328.
11. Park, H. S. Surface Stress Effects on the Resonant Properties of Silicon Nanowires. *J. Appl. Phys.* **2008**, *103*, 123504.
12. Park, H. S.; Klein, P. A. Surface Cauchy-Born Analysis of Surface Stress Effects on Metallic Nanowires. *Phys. Rev. B* **2007**, *75*, 085408.

13. Cuenot, S.; Frétigny, C.; Demoustier-Champagne, S.; Nysten, B. Surface Tension Effect on the Mechanical Properties of Nanomaterials Measured by Atomic Force Microscopy. *Phys. Rev. B* **2004**, *69*, 165410.
14. Jing, G. Y.; Duan, H. L.; Sun, X. M.; Zhang, Z. S.; Xu, J.; Li, Y. D.; Wang, J. X.; Yu, D. P. Surface Effects on Elastic Properties of Silver Nanowires: Contact Atomic-Force Microscopy. *Phys. Rev. B* **2006**, *73*, 235409.
15. Wong, E. W.; Sheehan, P. E.; Lieber, C. M. Nanobeam Mechanics: Elasticity, Strength and Toughness of Nanorods and Nanotubes. *Science* **1997**, *277*, 1971–1975.
16. Salvetat, J.-P.; Briggs, G. A. D.; Bonard, J.-M.; Bacsa, R. R.; Kulik, A. J.; Stöckli, T.; Burnham, N. A.; Forró, L. Elastic and Shear Moduli of Single-Walled Carbon Nanotube Ropes. *Phys. Rev. Lett.* **1999**, *82*, 944–947.
17. Tombler, T. W.; Zhou, C.; Alexseyev, L.; Kong, J.; Dai, W.; Liu, L.; Jayanthi, C. S.; Tang, M.; Wu, S.-Y. Reversible Electromechanical Characteristics of Carbon Nanotubes under Local-Probe Manipulation. *Nature* **2000**, *405*, 769–772.
18. Pennelli, G.; D'Angelo, F.; Piotto, M.; Barillaro, G.; Pellegrini, B. A Low Cost High Resolution Pattern Generator for Electron-Beam Lithography. *Rev. Sci. Instrum.* **2003**, *74*, 3579–3582.
19. Pennelli, G.; Pellegrini, B. Fabrication of Silicon Nanostructures by Geometry Controlled Oxidation. *J. Appl. Phys.* **2007**, *101*, 104502.
20. Pennelli, G. Top Down Fabrication of Long Silicon Nanowire Devices by Means of Lateral Oxidation. *Microelectron. Eng.* **2009**, *86*, 2139–2143.
21. Tiberj, A.; Fraisse, B.; Blanc, C.; Contreras, S.; Camassel, J. Process-Induced Strain in Silicon-on-Insulator Materials. *J. Phys.: Condens. Matter* **2002**, *14*, 13411–13416.
22. Park, S.; Kwak, D.; Ko, H.; Song, T.; il Cho, D. Selective Silicon-on-Insulator (SOI) Implant: A New Micromachining Method without Footing and Residual Stress. *J. Micromech. Microeng.* **2005**, *15*, 1607–1613.
23. Timoshenko, S., Goodier, J. N., Eds. *Theory of Elasticity*; Mc-Graw Hill: Cambridge, 1951.
24. Miller, R. E.; Shenoy, V. B. Size-Dependent Elastic Properties of Nanosized Structural Elements. *Nanotechnology* **2000**, *11*, 139–147.
25. Shenoy, V. B. Atomistic Calculations of Elastic Properties of Metallic fcc Crystal Surfaces. *Phys. Rev. B* **2005**, *71*, 094104.
26. Muller, P.; Saú, A. Elastic Effects on Surface Physics. *Surf. Sci. Rep.* **2004**, *54*, 157–258.